IEEE Access
Multidisciplinary | Rapid Review | Open Access Journal

Received June 5, 2020, accepted June 18, 2020, date of publication June 24, 2020, date of current version July 6, 2020.

Digital Object Identifier 10.1109/ACCESS.2020.3004731

Efficient Reconstruction Technique for Multi-Slice CS-MRI Using Novel Interpolation and 2D Sampling Scheme

MARIA MURAD[1], MUHAMMAD BILAL[1], ABDUL JALIL[1], AHMAD ALI[2], KHIZER MEHMOOD[1], AND BABER KHAN[1]

[1]Department of Electrical Engineering, International Islamic University Islamabad, Islamabad 44000, Pakistan
[2]Department of Software Engineering, Bahria University, Islamabad 44000, Pakistan

Corresponding author: Maria Murad (maria.murad@iiu.edu.pk)

ABSTRACT Compressed Sensing (CS) theory breaks the Nyquist theorem through random under-sampling and enables us to reconstruct a signal from 10%-50% samples. Magnetic Resonance Imaging (MRI) is a good candidate for application of compressed sensing techniques due to i) implicit sparsity in MR images and ii) inherently slow data acquisition process. In multi-slice MRI, strong inter-slice correlation has been exploited for further scan time reduction through interpolated compressed sensing (iCS). In this paper, a novel fast interpolated compressed sensing (FiCS) technique is proposed based on 2D variable density under-sampling (VRDU) scheme. The 2D-VRDU scheme improves the result by sampling the high energy central part of the k-space slices. The novel interpolation technique takes two consecutive slices and estimates the missing samples of the target slice (T slice) from its left slice (L slice). Compared to the previous methods, slices recovered with the proposed FiCS technique have a maximum correlation with their corresponding original slices. The proposed FiCS technique is evaluated by using both subjective and objective assessment. In subjective assessment, our proposed technique shows less partial volume loss compared to existing techniques. For objective assessment different performance metrics, such as structural similarity index measurement (SSIM), peak signal to noise ratio (PSNR), mean square error (MSE) and correlation, are used and compared with existing interpolation techniques. Simulation results on knee and brain dataset shows that the proposed FiCS technique has improved image quality and performance with even reduced scan time, lower computational complexity and maximum information content.

INDEX TERMS Compressed sensing, compressed sensing reconstruction, interpolated compressed sensing, magnetic resonance imaging, multi-slice MRI, nonlinear conjugate gradient.

I. INTRODUCTION

Magnetic Resonance Imaging (MRI) is a highly useful medical imaging technique for clinical diagnosis and research because it generates a very detailed picture of an inside body organ, without using any damaging ionizing radiations. The scan time of an MRI acquisition mainly depends on the raw k-space or Fourier data which are to be acquired to fulfill the Nyquist criteria [1]. Multiple lines of k-space are required to generate a single slice and Multi-slice MRI needs hundreds of such slices for just one MRI scan [2]. The speed of the data acquisition in MRI is fundamentally slow because of physical (gradient amplitude and slew-rate) and physiological (nerve stimulation) constraints. This slow imaging process of MRI may heighten the feelings of claustrophobia due to being in an enclosed space for prolonged durations, especially for pediatric. Secondly, it is very difficult for a patient to remain motionless and even held their breath for abdominal and cardiac scans, for that long [2], [3]. This slow imaging process can be accelerated using multiple coils that work in parallel called Parallel MRI (pMRI) [4]–[12]. But multiple coils require parallel imaging techniques, like sensitivity encoding (SENSE) and generalized autocalibrating partial parallel acquisition (GRAPPA) for the reconstruction of artifact-free images [9].

A. RELATED WORK

To reduce the scan time of MRI, another technique that has been evolved in recent years is Compressed Sensing (CS).

The associate editor coordinating the review of this manuscript and approving it for publication was Trivikram Rao Molugu.

Compressed Sensing enables the reconstruction of an image from even a fraction of the Nyquist samples, provided the basic constraints of CS are fulfilled [13]–[17]. For the implementation of CS, the three fundamental conditions are that the data must be sparse itself or in some transform domain, under-sampling must be done randomly and that the reconstruction must be performed using some non-linear techniques [18]–[20]. The random under-sampling transforms the CS reconstruction problem to de-noising because random under-sampling generates noise-like effects rather than aliasing [19]. CS is successfully applicable on MRI because MRI satisfies its basic requirements [21]. CS-MRI has the potential to improve patient care by reducing MRI acquisition times and enabling higher resolution imaging in clinically-acceptable scan times. With the edge of this reduced scan time, CS-MRI has additional computational overhead compared to standard MRI where only inverse Fourier transform is enough [22].

The CS-MRI trends can be broadly categorized as methods focused on improving the reconstruction strategies [23], [24], and parallel CS-MRI techniques [25]. For successful CS-MRI, the sparse regularization can be achieved in a specific transform domain or using some dictionary learning techniques [26]–[31]. The classic CS-MRI uses fixed sparsifying transforms like total variation (TV) [32], discrete cosine transforms (DCT) and discrete wavelet transforms (DWT) [33]. On the other hand, with the rapid development of deep learning, many CNN-based super-resolution (SR) methods [34]–[36] have also gained attention in recent years.

In CS-MRI all slices should be equally under-sampled and are then recovered using some non-linear reconstruction algorithms [2], [13], [37]. For an efficient reconstruction, the number of k-space samples should be roughly two to five times the number of sparse coefficients [19]. Thus for a good CS-MRI scan, at least 10% of the samples should be acquired from each slice for efficient reconstruction. In Multi-slice MRI there is a very narrow inter-slice gap, and therefore has a very strong inter-slice correlation. This correlation has been used in the literature to reduce the average samples per slice. Pang and Zhang [38], [39] exploits this correlation and introduced a new concept called interpolated Compressed Sensing (iCS) in MRI.

In Interpolated Compressed Sensing MRI (iCS-MRI), some of the CS samples are acquired and others and intentionally missed to reduce the average sampling rate, next the missed sampled are estimated from the samples of the neighboring slices [38]–[41]. The under-sampling can be performed using different sampling patterns like Cartesian, radial, spiral, and golden-angle [42]–[44]. Similarly, interpolation for the missing samples in the under-sampled slices can be accomplished using different interpolation techniques [38], [39], [41], [45], [46]. The last step of iCS can be carried out using one of the CS reconstruction techniques like Non-linear Conjugate Gradient (NCG) [19], Wavelet Tree Sparsity (WaTMRI) [47]–[49], Fast Composite Splitting Algorithm (FCSA) [50], and Iteratively weighted Wavelet Tree sparsity MRI (IWTMRI) [46]. Recently proposed [51] CS reconstruction algorithm has improved results with radial sampling. The CS reconstruction techniques vary in computational complexity, convergence time, and reconstructed image quality.

Pang and Zhang [39], utilizes 9% average samples. He reduced the average sampling rate by acquiring some slice as lightly under-sampled (L slices) and other as highly under-sampled (H slices). But his proposed interpolation technique is computationally inefficient with inconsistency in slice-wise reconstructed image quality. Hirabayashi *et al.* [52] use iCS by taking a different under-sampled slices sequence using fully sampled and CS slices (F and C slices). But his technique has rather increased the average sampling ratio.

Deka and Datta [10], Datta *et al.* [45], Datta and Deka [46], [53]–[55] further explored iCS-MRI with different interpolation and reconstruction strategies. Although they reduced the computational cost of their interpolation algorithms [45], [46] but they neither work on reducing the average sampling ratios nor on the consistency of their results. They used the same under-sampling strategy in their work [46] as proposed by pang and Zhang [39], but using a 1D mask. They also explored iCS for pMRI in [10], [55]. Their recent work [54] has further reduced the computational complexity but has rather increased the average sampling ratio. The sampling and interpolation strategy adopted in [39], [46] takes three consecutive slices with a specific under-sampling pattern of different sampling ratios and repeats that pattern after every three slices. The sampling pattern is such that the central slice is always lightly under-sampled and the two neighboring (Left and Right slices) are highly under-sampled. The main drawback of this non-uniform sampling strategy is that every three consecutive slices are more likely to be identical to the centered slice, after reconstruction. Hence in every three consecutive slices, the centered slice will always dominate the two neighboring slices. Secondly, this non-uniform sampling strategy loss most of the information in two out of the three consecutive slices. Different sampling strategies [37], [42], [44] have also been explored in iCS, but they neither reduced the scan time nor the average sampling ratio.

B. OUR CONTRIBUTION

In this work, the authors use a novel Fast Interpolated Compressed Sensing (FiCS) technique using 2D-VRDU sampling and a fast interpolation scheme. The proposed FiCS technique reduces the average under-sampling ratio, thus decreases the acquisition time. The proposed technique shows improved results with even 5% average samples thus reduces the sampling ratio and scan time. Secondly, the interpolation technique is computationally efficient with only a set difference and addition operation. The main advantage of the proposed FiCS technique is that for reconstruction consecutive under-sampled slices retains maximum samples of the original slices. Thus the resulting reconstructed images have maximum correlation with the original images. In the previous iCS

techniques [39], [46] most of the slices are more correlated to their neighboring slices, rather than their original ones.

The main contributions of this work are a reduction in scan time by employing higher under-sampling rates while improving image quality and consistency by applying a more uniform under-sampling strategy in each slice.

C. PAPER OUTLINE

The rest of the paper is organized as follows. In Section II interpolated Compressed Sensing is discussed, in Section III the proposed algorithm is explained, in Section IV simulation and results are presented followed by discussion and conclusion in Section V and future work in Section VI.

II. INTERPOLATED COMPRESSED SENSING (iCS)

Interpolated Compressed Sensing (iCS) reconstructs images from under-sampled k-space data with even reduced sampling ratios compared to CS. Interpolated Compressed Sensing works in three steps; first, it under-samples the slices, second interpolates the missing samples, and lastly reconstruction using CS, as shown in Fig. 1.

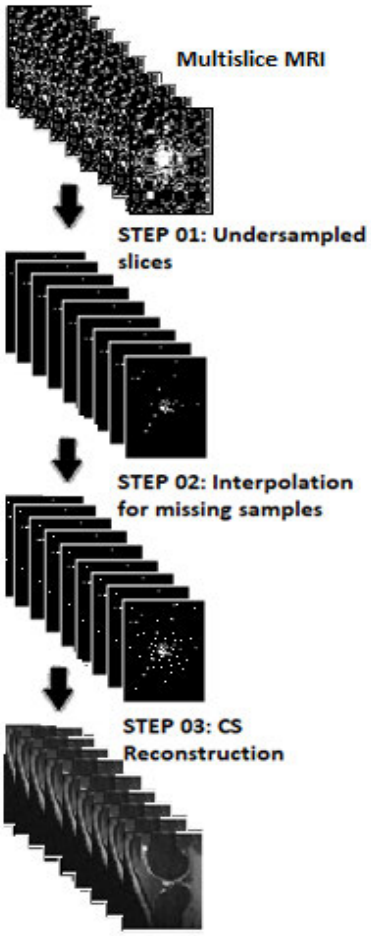

FIGURE 1. Three steps of iCS.

In the first step, the under-sampling is performed by intentionally missing some of the CS samples. In the second step, those missed samples are estimated from the neighboring slices using interpolation to get CS slices. Finally, CS reconstruction is applied using one of the CS reconstruction algorithms.

Recent researchers propose iCS with 9% average under-sampling ratio [39], [46]. Their under-sampling pattern of the three consecutive slices, which repeats after every three slices, is shown in Fig. 2. It is clear from the figure that, in three consecutive slices, the first one is highly under-sampled (H slice), second is lightly under-sampled (L slice) and the third is again H slice, for both 1D and 2D-VRDU schemes. Each H and L slice has 1 % and 25% of the total samples respectively. Therefore the average sampling ratio for this scheme is 9%. The H slice missed samples are interpolated from the neighboring L slice to get H interpolated slice with 25 % samples. Finally, CS reconstruction is applied to all the H interpolated and L slices.

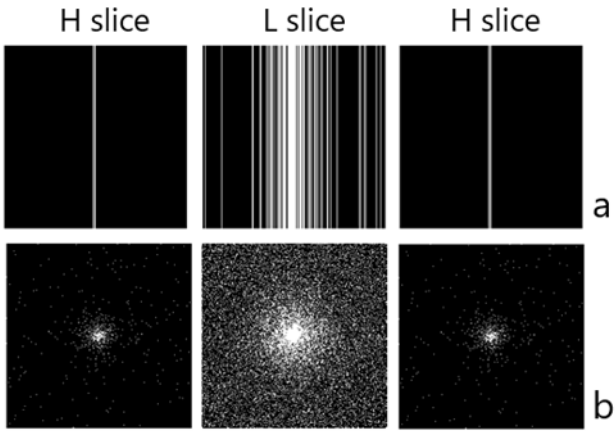

FIGURE 2. (a) 1D (b) 2D-VRDU sampling patterns for three consecutive slices.

The main drawback of this non-uniform sampling strategy is that H slice 1% samples are insufficient to be called an original image after interpolation and reconstruction. Thus in every three consecutive slices, the L slice will always dominate their two neighboring H slices. This results in almost the same imaging information in every three consecutive reconstructed slices.

Pang and Zhang [39] have worked on 2D-VRDU where Datta and Deka [46] on 1D-VRDU. The interpolation technique of both the sampling schemes (1D and 2D) has complex computational steps of Fourier, Inverse Fourier, matrix division, and convolution resulting in increased computational cost along with inaccuracy in their results. Datta in his recent work [46] claims improved results, therefore we have compared our proposed FiCS technique with their work for both 1D and 2D sampling schemes.

III. PROPOSED ALGORITHM

The proposed Fast interpolated Compressed Sensing (FiCS) algorithm works in three steps. Each step is discussed separately in subsections.

A. 2D-VRDU SAMPLING SCHEME

The original k-space or Fourier data of multi-slice MRI sequence has maximum energy points at the center which resembles a 2D-VRDU pattern, as shown in Fig. 3. Therefore the same 2D sampling pattern is adopted in this research because it can efficiently under-sample the original k-space data from a multi-slice MRI sequence.

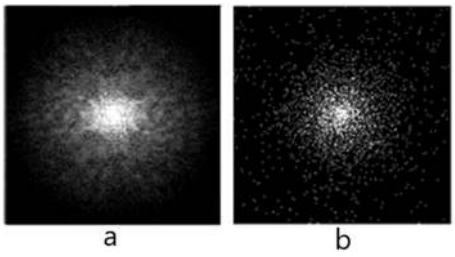

FIGURE 3. (a) Full k-space data and (b) under-sampled k space data acquired using a 2D-VRDU mask.

The sampling strategy used in this research takes only 5%, 2D-VRDU samples, from each slice of a multi-slice sequence. First two such masks with 5%, samples are generated using 2D Gaussian PDF. Then these masks are used for under-sampling of two consecutive slices and repeated after every two slices. Two such masks are shown in Fig. 4.

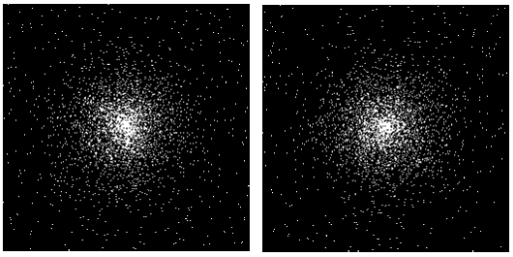

FIGURE 4. The proposed sampling pattern for two consecutive slices.

Two fully sampled original multi-slice MRI data sets are used in this research. Before applying the proposed FiCS technique, the multi-slice MRI sequence is first under-sampled into k-space data. For under-sampling of an i^{th} slice $\boldsymbol{S_i}$, first a down-sampling Fourier operator $\boldsymbol{F_u}$ of the proposed sampling pattern is generated. Then $\boldsymbol{F_u}$ is applied on $\boldsymbol{S_i}$, resulting in an under-sampled slice $\boldsymbol{U_i}$, in k space as represented in (1).

$$\boldsymbol{U_i} = \boldsymbol{F_u} * \boldsymbol{S_i} \tag{1}$$

This step is repeated for each slice of the multi-slice sequence using the proposed sampling patterns of Fig. 4 for two consecutive slices and repeated for the whole dataset. As clear from Fig. 4, both 2D-VRDU masks have the same sampling pattern but different sampling locations. A detailed examination of both the under-sampling patterns reveals that any two such generated masks will always have 72% samples on different locations and rest 28% on identical locations. The sampling points on different locations will be exploited for the proposed interpolation scheme in the next step.

B. PROPOSED FAST INTERPOLATION SCHEME

The proposed fast interpolation technique estimates the missing samples in each under-sampled slice $\boldsymbol{U_i}$ of the multi-slice MRI sequence. This scheme works by taking two consecutive slices, in which the first one is called Left slice (L slice) and the second one is called Target slice (T slice). The $\boldsymbol{T}$ slice will always be interpolated from its $\boldsymbol{L}$ slice. The proposed interpolation scheme has two steps. The first step is the set difference between $\boldsymbol{L}$ and $\boldsymbol{T}$ slices as shown in (2). The resultant difference between the two slices is called $\boldsymbol{T_{new}}$, containing the new sampling information which was missed from $\boldsymbol{T}$ slice.

$$\boldsymbol{T_{new}} = \boldsymbol{L} \ominus \boldsymbol{T} \tag{2}$$

where the $\ominus$ sign shows set difference operator. Both $\boldsymbol{L}$ and $\boldsymbol{T}$ slices have 5% 2D-VRDU samples, therefore their set difference $\boldsymbol{T_{new}}$, will have 3.6% samples. In the second step these 3.6% samples of $\boldsymbol{T_{new}}$ are combined with 5% samples of $\boldsymbol{T}$ slice resulting in 8.6% samples in the interpolated $\boldsymbol{T}$ slice called $\boldsymbol{T_{int}}$ as shown in (3), where the $\oplus$ sign shows set addition operation.

$$\boldsymbol{T_{int}} = \boldsymbol{T_{new}} \oplus \boldsymbol{T} \tag{3}$$

This two-step interpolation technique is applied on all the slices of under-sampled multi-slice sequence, considering each slice as $\boldsymbol{T}$ and its preceding as $\boldsymbol{L}$ slice, to get interpolated slices, $\boldsymbol{T_{int}}$. The complete two step approach of the proposed interpolation technique is shown in Fig. 5. For current clinical scanners, the same sampling strategy has also been implemented using 1D-VRDU masks.

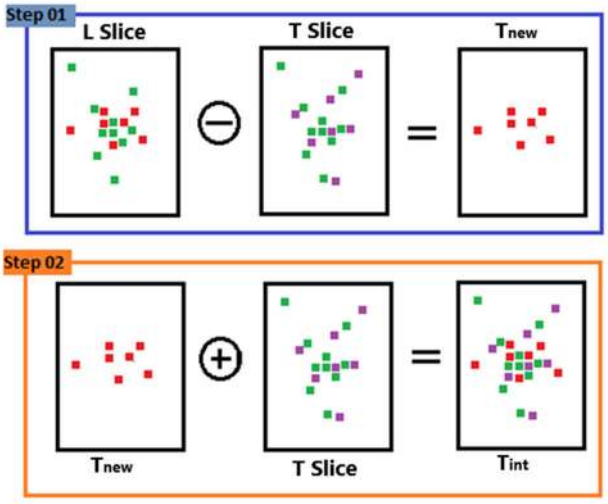

FIGURE 5. The proposed fast interpolation technique.

As shown in Fig. 5 this interpolation process only includes a set difference and addition operation. No complex computations of Fourier, Inverse Fourier, convolution and matrix division are used compared to the recent techniques [39], [45], [46]. Therefore the computational complexity of the proposed algorithm is O(n), compared to $O(n^2)$ in [39] and O(n log n) in [46].

C. CS RECONSTRUCTION

After interpolation, the next step is to apply CS reconstruction to get the reconstructed images. The CS reconstruction algorithm uses a non-linear conjugate gradient (NCG) with ℓ_1-norm and Total Variance (TV) [19] as shown in (4).

$$\hat{x} = arg \min_{x} \|F_u x - y\|_2^2 + \lambda_1 \|\Psi x\|_1 + \lambda_2 \|x\|_{TV} \quad (4)$$

Thus for a given k-space measurement y and a down-sampled Fourier operator F_u, the function reconstructs the image x that minimizes the cost function with the given ℓ_1-norm and TV constraints, where Ψ represents the wavelet operator. The objective function is ℓ_1-norm which is defined as $\|x\|_1 = \sum_i |x_i|$ and minimizing $\|\Psi x\|_1$ promotes sparsity. Similarly the constraint $\|F_u x - y\|_2^2$ enforces data consistency. Where λ_1 and λ_2 are ℓ_1 wavelet penalty and TV penalty respectively. The TV is defined discretely in (5).

$$\|x\|_{TV} = \sum_{i,j} \left[(\nabla_1 x_{ij})^2 + (\nabla_2 x_{ij})^2 \right] \quad (5)$$

where ∇_1 and ∇_2 denotes the forward finite difference operators on the first and second coordinates respectively. The complete process of the proposed FiCS scheme is shown in Fig. 6.

IV. SIMULATION AND RESULTS

The proposed Fast iCS (FiCS) has been evaluated on two different data sets. The knee data set is taken from a free online database, http://mridata.org. This is a fully sampled data set acquired from a GE HD 3T scanner with $160 \times 160 \times 153.6$ mm field of view, number of channels: 8, matrix size: 320×320 with 256 slices, slice thickness 0.6mm, zero inter-slice gap, TR/TE: 1150/25 msec, flip angle 90, and bandwidth 50kHz. The brain data set is of normal aging coronal plane with 123 slices, matrix size: 256×256, and is publicly available on AANLIB database of Harvard medical school at http://www.med.harvard.edu/AANLIB/home.html [56].

To evaluate the performance of the proposed FiCS algorithm the simulation results are obtained using MATLAB 2016-a, with 2.6 GHz Intel core i7, 64 bit operating system and 16 GB RAM.

A. EVALUATION CRITERIA

To assess the quality of the reconstructed images two methods are used: subjective and objective. The subjective method is based on the perceptual assessment of radiologists about the attributes of the reconstructed data sets, while objective methods are based on computational models that can predict perceptual image quality. Similarly, hybrid methods like SIS (semantic interpretability score) [57] are also very useful for both subjective and objective assessment.

For subjective assessment we asked some expert radiologists to assess the reconstructed datasets. The rating is based on the overall quality and information content of the images. The images reconstructed using the proposed FiCS shows lesser partial volume loss compared to iCS.

For objective assessment four assessment parameters are used to evaluate and compare our proposed FiCS technique with recent interpolation technique [46] and CS [19]. These parameters are Structural Similarity Index Measurement (***SSIM***) [58], Mean Square Error (***MSE***) [59], Peak Signal to Noise Ratio (***PSNR***) [59] and correla-

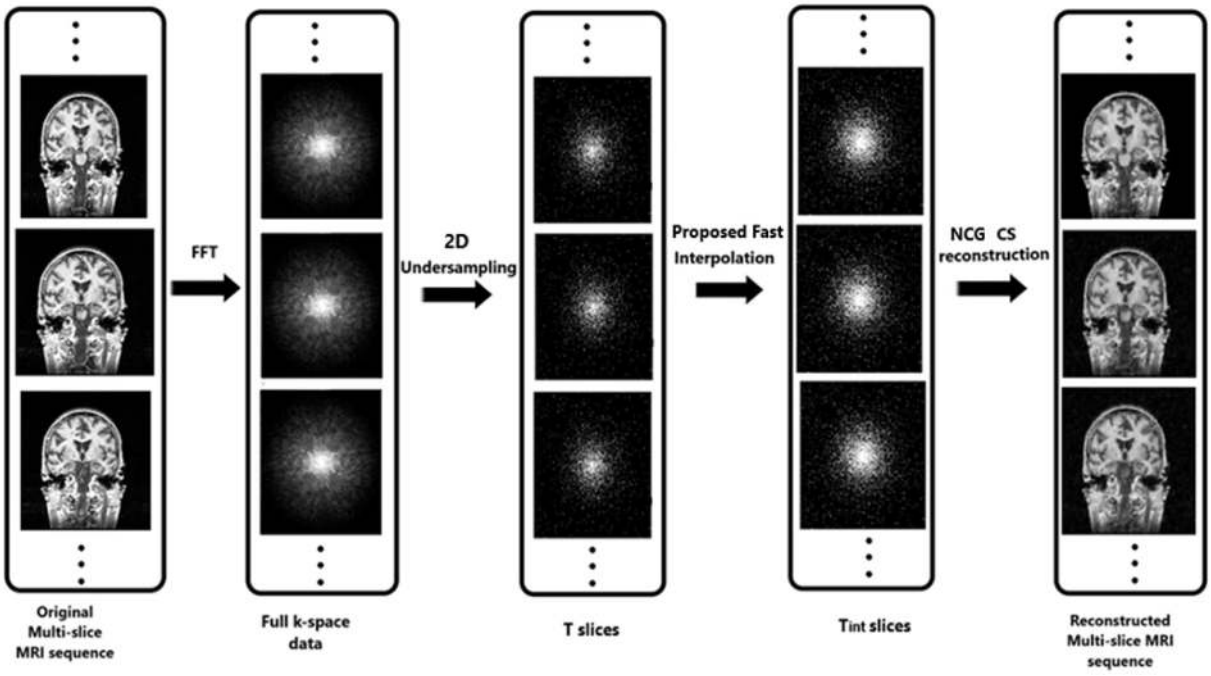

FIGURE 6. Proposed FiCS scheme.

tion (***CORR***) [60], their mathematical description is given in (6)-(9).

$$SSIM\,(x,y) = \frac{(2\mu_x\mu_y + c_1)\,(2\sigma_{xy} + c_2)}{\left(\mu_x^2 + \mu_y^2 + c_1\right)\left(\sigma_x^2 + \sigma_y^2 + c_2\right)} \tag{6}$$

$$MSE = \frac{1}{mn}\sum_{i=0}^{m-1}\sum_{j=0}^{n-1}[x\,(i,j) - y\,(i,j)]^2 \tag{7}$$

$$PSNR = (in\ dB) = 10log_{10}\frac{(MAX_x)^2}{MSE} \tag{8}$$

$$CORR = \frac{\sum_{i,j}\{[x(i,j) - \mu_x][y(i,j) - \mu_y]\}}{\sqrt{\left\{\sum_{i,j}[x(i,j) - \mu_x]^2\right\}\left\{\sum_{i,j}[y\,(i,j) - \mu_y]^2\right\}}} \tag{9}$$

where $\boldsymbol{x}$ and $\boldsymbol{y}$ are the original and reconstructed images of size $\boldsymbol{m \times n}$. $\boldsymbol{\mu_x}$ and $\boldsymbol{\mu_y}$ are the mean values, $\boldsymbol{\sigma_x^2}$ and $\boldsymbol{\sigma_y^2}$ denotes the variances and $\boldsymbol{\sigma_{xy}}$ represents the covariance of $\boldsymbol{x}$ and $\boldsymbol{y}$. $\boldsymbol{c_1 = (k_1 L)^2}$ and $\boldsymbol{c_1 = (k_2 L)^2}$ are the variables to stabilize the division, where $\boldsymbol{k_1}$ and $\boldsymbol{k_2}$ are small constants and $\boldsymbol{L}$ is the dynamic range of the image.

B. EVALUATION OF THE UNDER-SAMPLING SCHEME

Like CS, our sampling strategy equally under samples all the slices of multi-slice MRI sequence. This gives us the main edge of our research that during interpolation most of the samples are retained from the original slices. Hence the reconstructed images have maximum information of the original images as shown in Fig. 7 and 8.

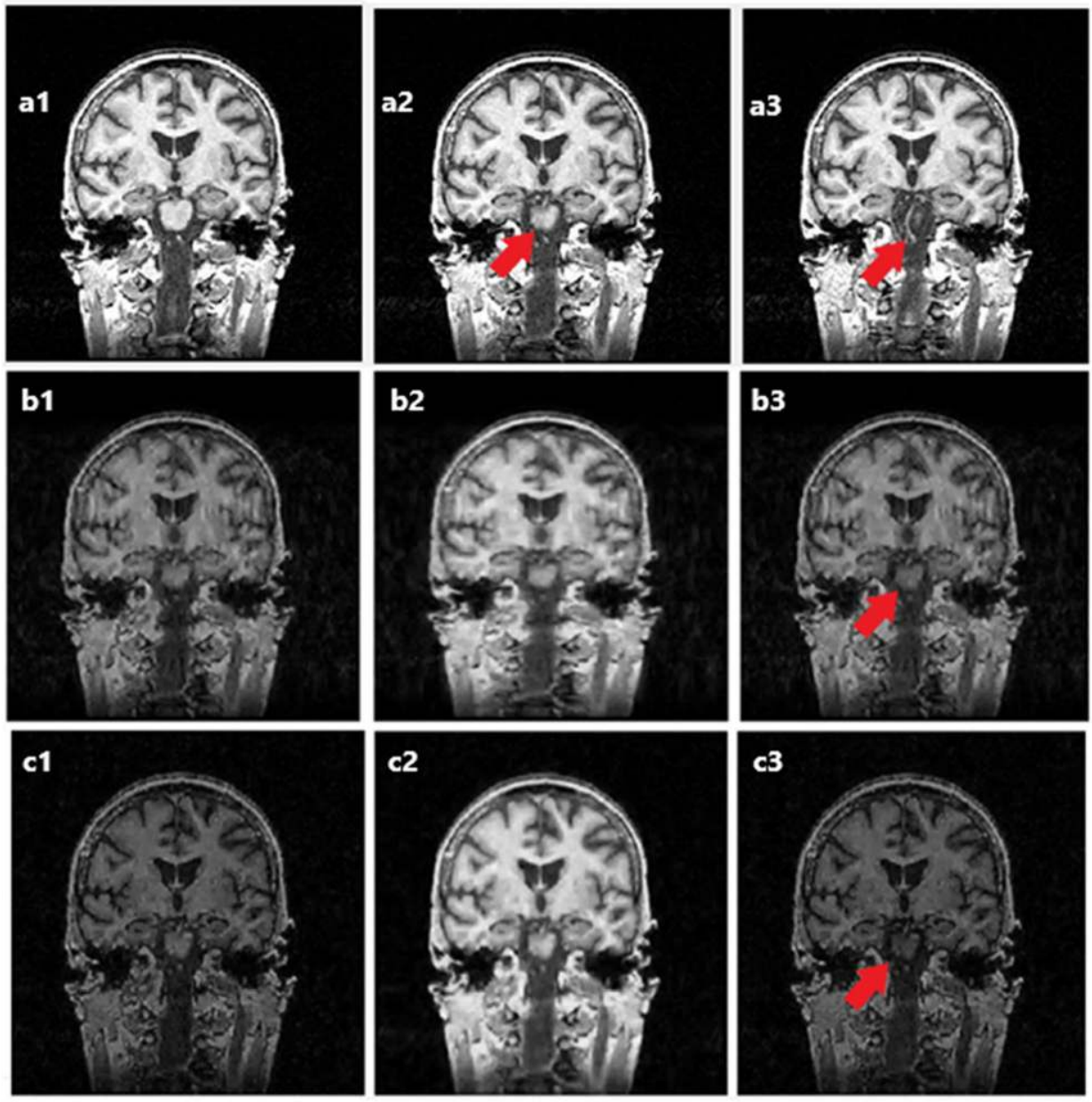

FIGURE 7. Three consecutive (a) original and reconstructed images using (b) iCS-1D and (c) iCS-2D. New information is pointed by the arrow in a3 which is missed by iCS in both b3 and c3. The three consecutive slices of iCS (b1-b3 and c1-c3) shows similar information to central slice (b2 and c2) and is the same as in the original centered slice (a2). Secondly, iCS also shows large contrast variation in adjacent slices.

The benefit of proposed sampling strategy to acquire the under-sampled $\boldsymbol{T}$ slices is that after interpolation every $\boldsymbol{T}_{int}$ slice will have 60% samples from $\boldsymbol{T}$ slice and rest 40% from its $\boldsymbol{L}$ slice. In the previous techniques [39], [46] each interpolated slice had only 4% samples from their original under-sampled slice and rest 96% from its neighboring slice. Thus their result is that every three consecutive reconstructed images represent the same information as shown in Fig.7 (b1-b3 and c1-c3). A Comparison of three consecutive original images with reconstructed images using iCS-1D and iCS-2D is shown in Fig. 7, while Fig. 8 shows comparison with FiCS-1D and FiCS-2D. It is clear from Fig.8 that the each reconstructed slice using FiCS has preserved the original information of their corresponding original slices. While in iCS two of the three consecutive slices have missed their original information and represent information of their neighboring centered slice. In short, the three consecutive slices of iCS are same in terms of the information content while our proposed FiCS has retained the information of the original respective slices.

Assessment of three consecutive slices of both knee and brain data sets, using the four parameters, are shown

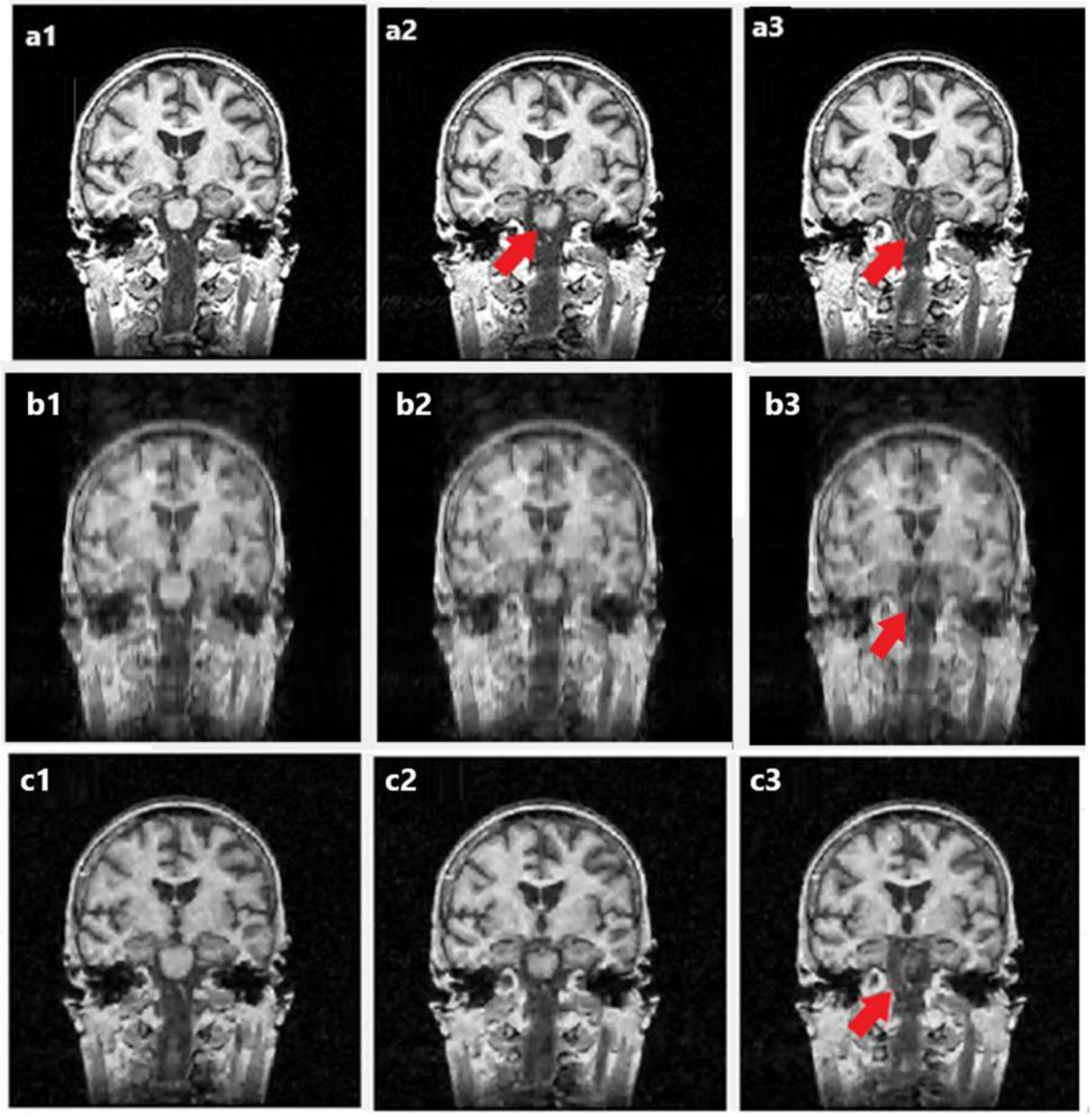

FIGURE 8. Three consecutive (a) original and reconstructed images using (b) FiCS-1D and (c) FiCS-2D. New information is pointed by the arrow in a3 which was missed by iCS, while FiCS has retained that information in both 1D (b3) and 2D (c3). Similarly, FiCS shows no contrast variation in adjacent slices while preserving the original information of their corresponding original slices.

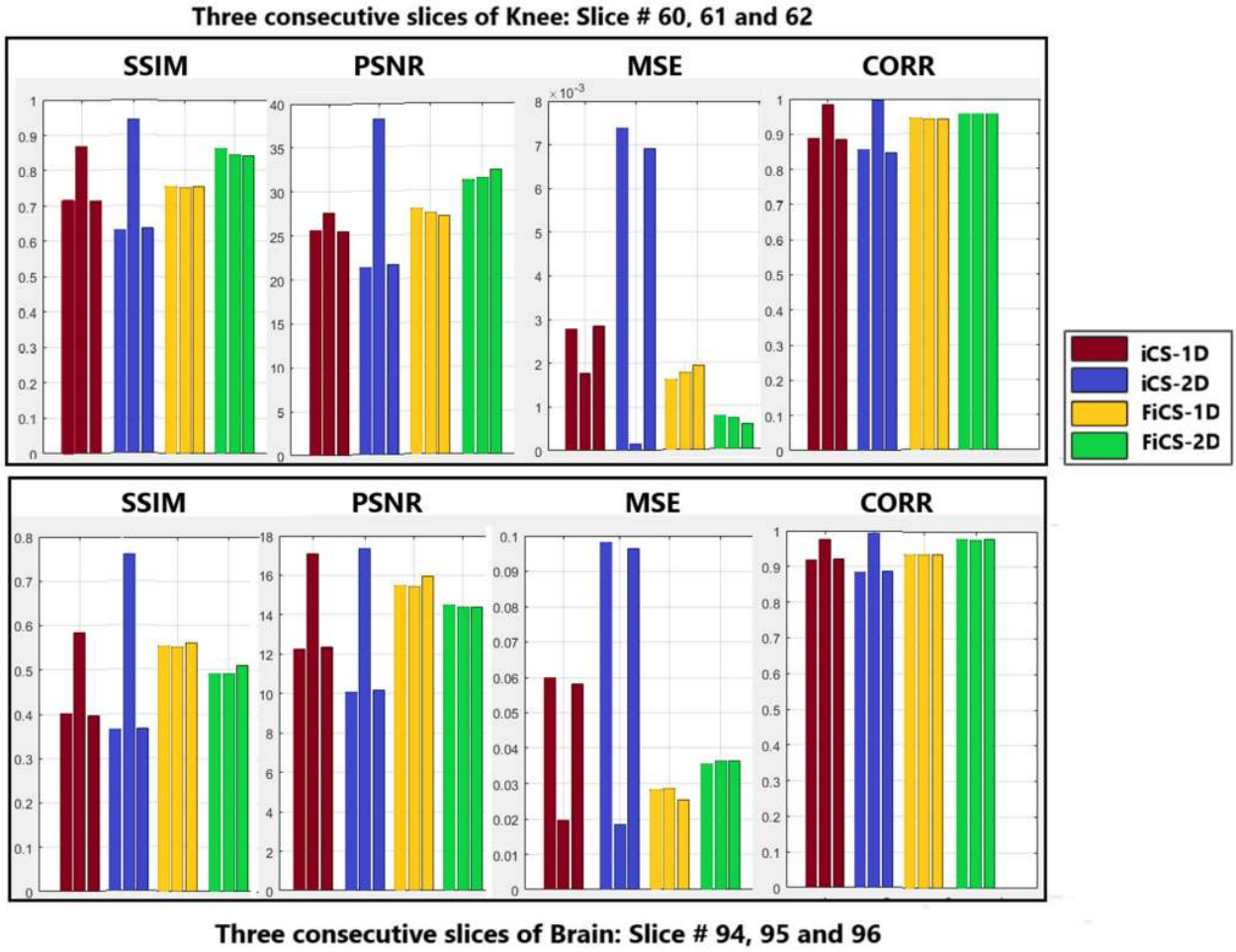

FIGURE 9. Slice-wise assessment of three consecutive slices on both knee and brain data sets. iCS-1D and iCS-2D shows huge variations in values while our proposed FiCS technique has consistent values in both 1D and 2D like CS and is better than CS.

in Fig. 9. This assessment is performed on iCS-1D, iCS-2D, FiCS-1D, and FiCS-2D using the same 9% average samples. As shown in the three consecutive reconstructed images of Fig. 7 (b1-b3 and c1-c3), iCS shows wide variation in terms of image quality and contrast. The same variation is verified through their assessment in Fig. 9, which shows huge variations in values. The assessment of FiCS, in Fig. 9, shows no such abrupt changes in values of three consecutive slices and the same is verified from Fig. 8 (b1-b3 and c1-c3). The centered slice in iCS Fig. 7 (b2 and c2) looks good and has improved assessment on all parameters, as shown in Fig. 9, because of the fact that it has 25% of the original samples while the proposed FiCS has only 9% of it. But this uneven distribution of under-sampling ratios in iCS results in every three consecutive slices to be same in terms of the imaging information. Thus iCS shows non-consistent results both qualitatively and quantitatively where FiCS shows consistent results.

C. EVALUATION OF THE PROPOSED FAST INTERPOLATION SCHEME

The proposed Fast interpolation scheme (FiCS) is evaluated by comparing the assessment parameters of FiCS with recent iCS [46] and CS [19] techniques for both 1D and 2D-VRDU masks. Fig. 10 shows the evaluation of all four assessment parameters using 9% average sampling ratios. For fair comparison, the assessment has been done on 9 consecutive slices and averaged. It is clear from the graph that although iCS technique with 1D-VRDU mask performed better than CS, as claimed by its authors [46]. But when the same is implemented with a 2D-VRDU mask it performs worse even from CS.

2D-VRDU mask is most capable to acquire the k-space data of a multi-slice MRI sequence, because of its resemblance with the original k-space data. Therefore a good iCS technique is one that performs better using 2D-VRDU masks. The proposed FiCS-2D outperforms all the other techniques on all the four assessment parameters. Although

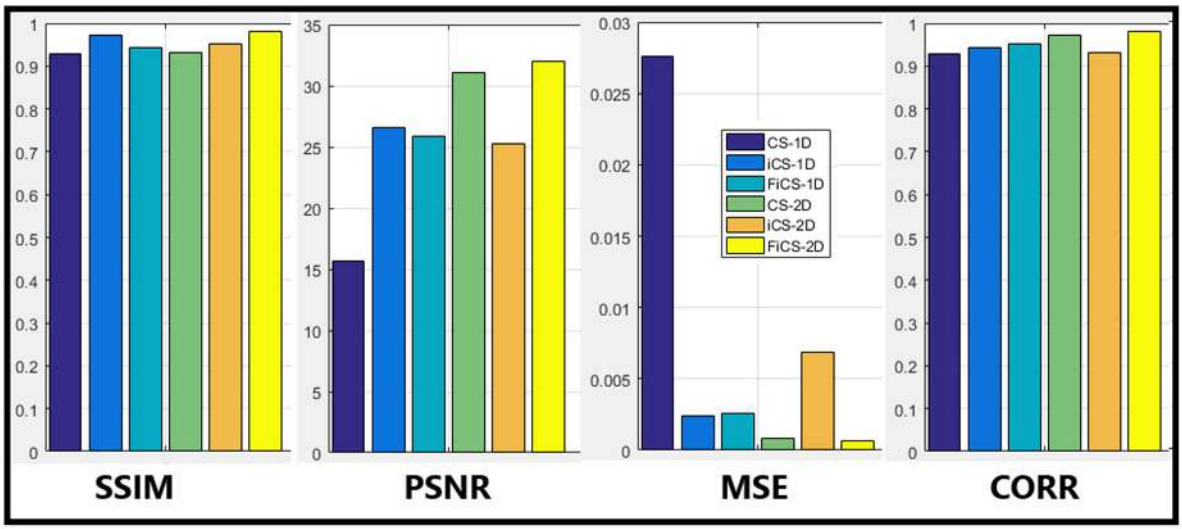

FIGURE 10. Four assessment parameters on knee data sets. Comparing CS-1D, iCS-1D, FiCS-1D, CS-2D, iCS 2D and FiCS-2D with 9% average sampling ratio. The assessment is done on 9 consecutive slices (slice number 74-82) and averaged. It is clear that FiCS-2D outperforms all on all the assessment parameters.

FiCS-1D also performs far better than iCS-1D on individual consecutive slices as shown in Fig. 9 but due to the uneven distribution of sampling ratios in iCS their average assessment of 9 consecutive slices are almost same as FiCS-1D.

For fair comparison selected zoomed parts of the original images of both knee and brain are also compared with the reconstructed images using CS, iCS and FiCS. The original image has 100% samples while the reconstructed images have 9% average samples as shown in Fig. 11. It is clear from the figure that our proposed FiCS technique has more clear results, compared to all other techniques. It is to be clarified that the reconstructed images of iCS (c, f and i, l) look sharper because it has been reconstructed using 25% samples, in which 1% samples are taken from the original slice and rest 24% from the neighboring slice. Therefore although their images look sharper but the information is not original. Secondly, the redundant Fourier steps in the interpolation of iCS [46] causes large contrast variation in their adjacent slices. Thus these extra Fourier steps not only makes their algorithm computationally complex but also cause huge contrast variations in consecutive reconstructed slices as shown in Fig. 7.

Most importantly the computational complexity of the proposed interpolation algorithm is reduced to O(n), compared to O(n log n) of iCS [46]. The processing time of the proposed fast interpolation technique is up to five times faster compared to the current interpolation technique [46].

The Proposed FiCS technique has not only improved performance with the same average sampling ratio (9%) but also outperforms with 7% and with even 5% sampling ratios as shown in Table 1. Similarly, the reconstructed images using 7% and 5% are also better than iCS with even half the sampling rate as shown in Fig. 12.

TABLE 1. Comparison of proposed FiCS-2D with 9%, 7% and 5% under-sampling ratios.

Knee Dataset, Average of 9 slices [74-82]						
S.No	**Assessment Parameter**	**iCS-1D-9%**	**iCS-2D-9%**	**FiCS-9%**	**FiCS-7%**	**FiCS-5%**
1	**SSIM**	0.7434	0.67581	**0.8551**	**0.831**	**0.7626**
2	**PSNR**	26.5709	25.2133	**32.021**	**30.71**	**29.4**
3	**MSE**	0.00239	0.00688	**0.0007**	**0.0009**	**0.0012**
4	**CORR**	0.94428	0.93285	**0.981**	**0.976**	**0.9654**

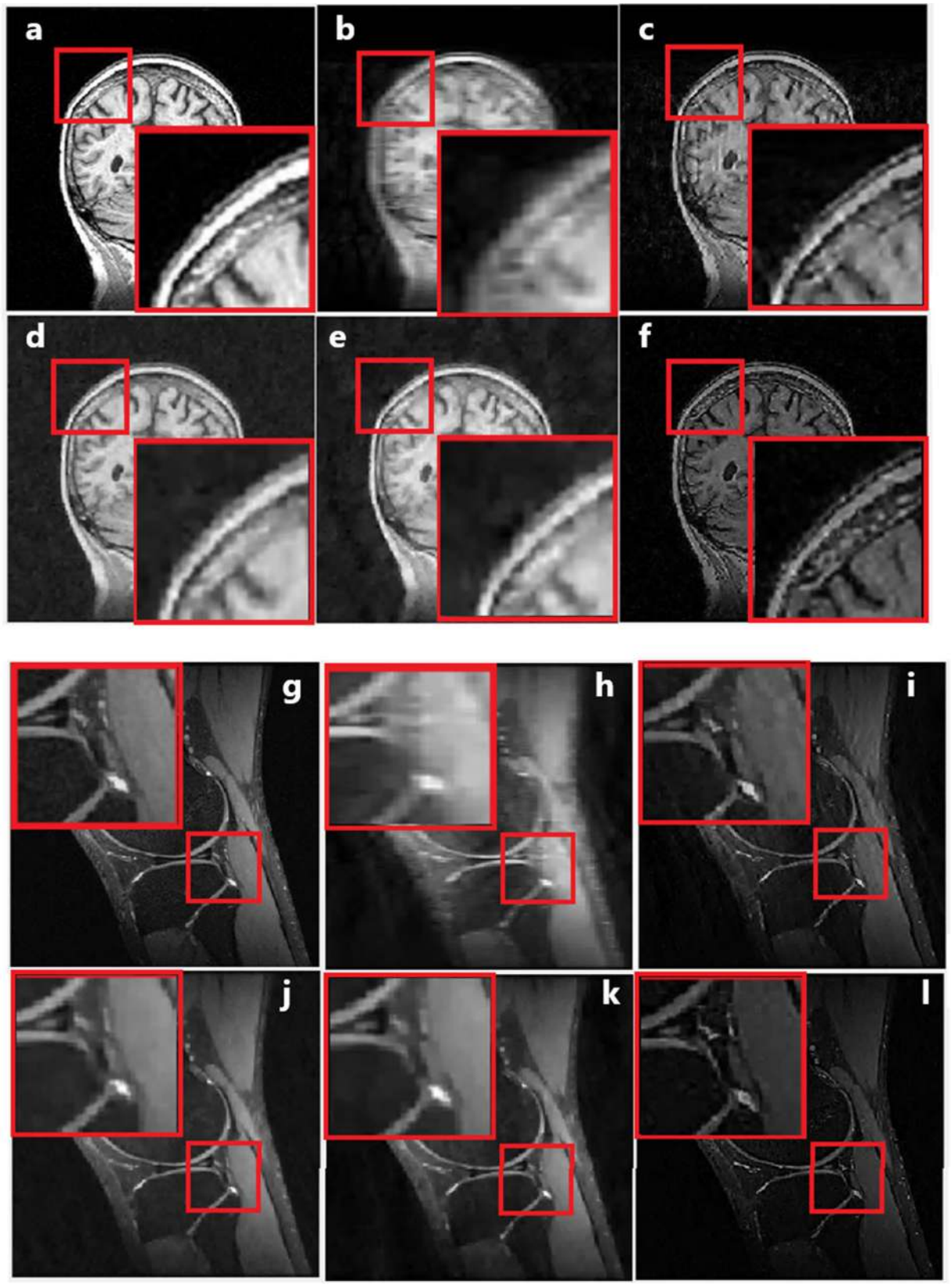

FIGURE 11. Comparison of (a) Original brain Image with Reconstructed images using (b) CS-1D, (c) iCS-1D, (e) CS-2D, (f) iCS-2D and (d) Proposed FiCS-2D with 9% average sampling ratio. Similarly, comparison of (g) Original knee Image with Reconstructed images using (h) CS-1D, (i) iCS-1D, (k) CS-2D, (l) iCS-2D and Proposed (j) FiCS-2D with 9% average sampling ratio. It is clear that the reconstructed image using the proposed technique has better quality compared to other techniques.

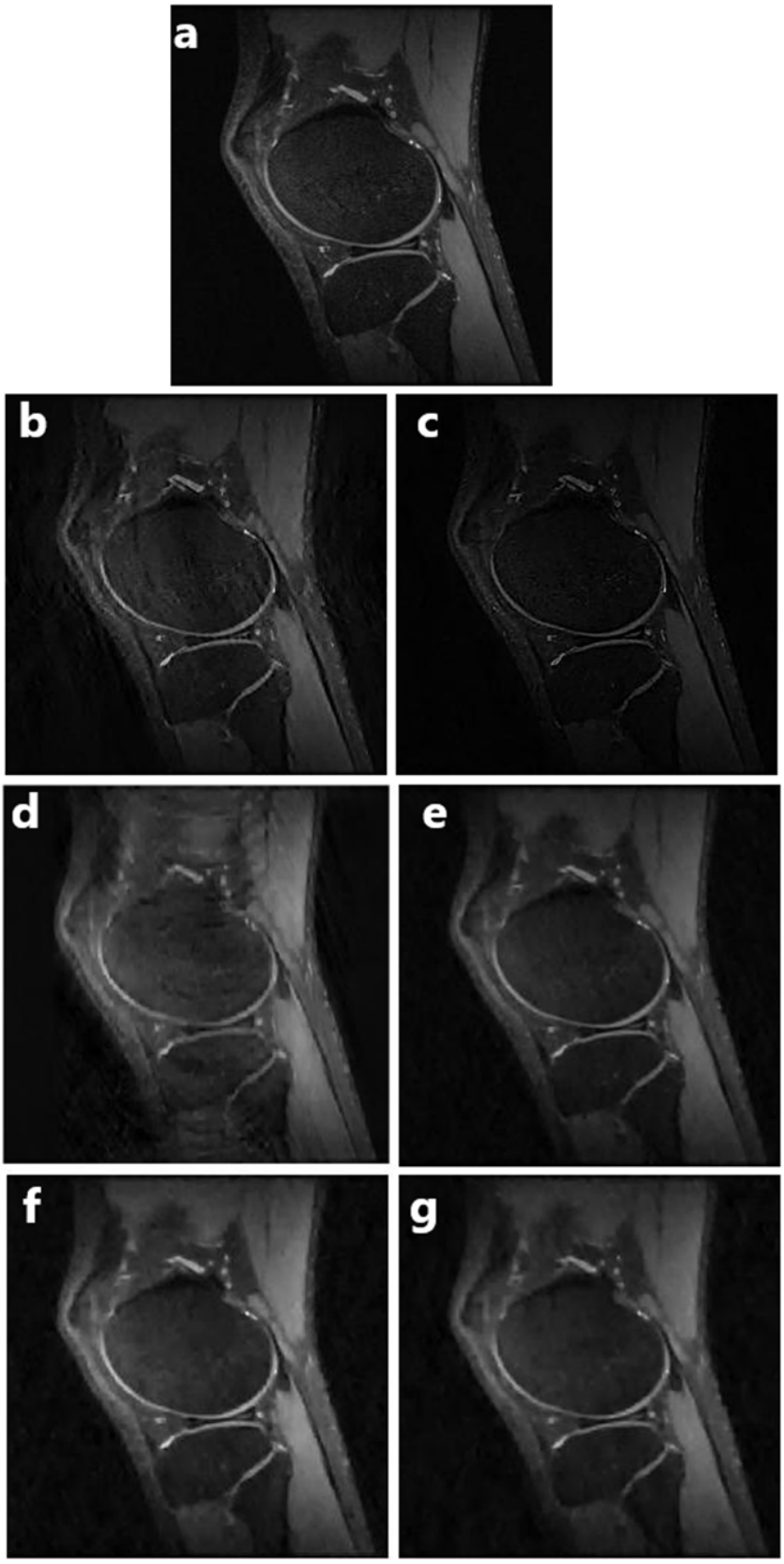

FIGURE 12. Comparison of (a) Original image with (b) iCS-1D- 9%, (c) iCS-2D- 9%, (d) FiCS-1D-9%, (e) FiCS-2D-9%, (f) FiCS-2D- 7% and (g) FiCS-2D-5%. The Proposed FiCS shows better results even 5% samples.

D. EVALUATION OF FiCS

The proposed FiCS technique is evaluated on centered 150 slices of knee data set (slice # 51 to 200) as shown in Fig. 13. It can be seen in the graphs that iCS-1D and 2D have huge fluctuation throughout the data set while FiCS follows a uniform pattern like CS, with improved results. The fluctuations in the graphs of iCS are such that it has peaks on the centered 25% slices and depressions on 1% (25% after interpolation) slices. While FiCS has no such biasing in sampling like CS and therefore has uniformity in their results.

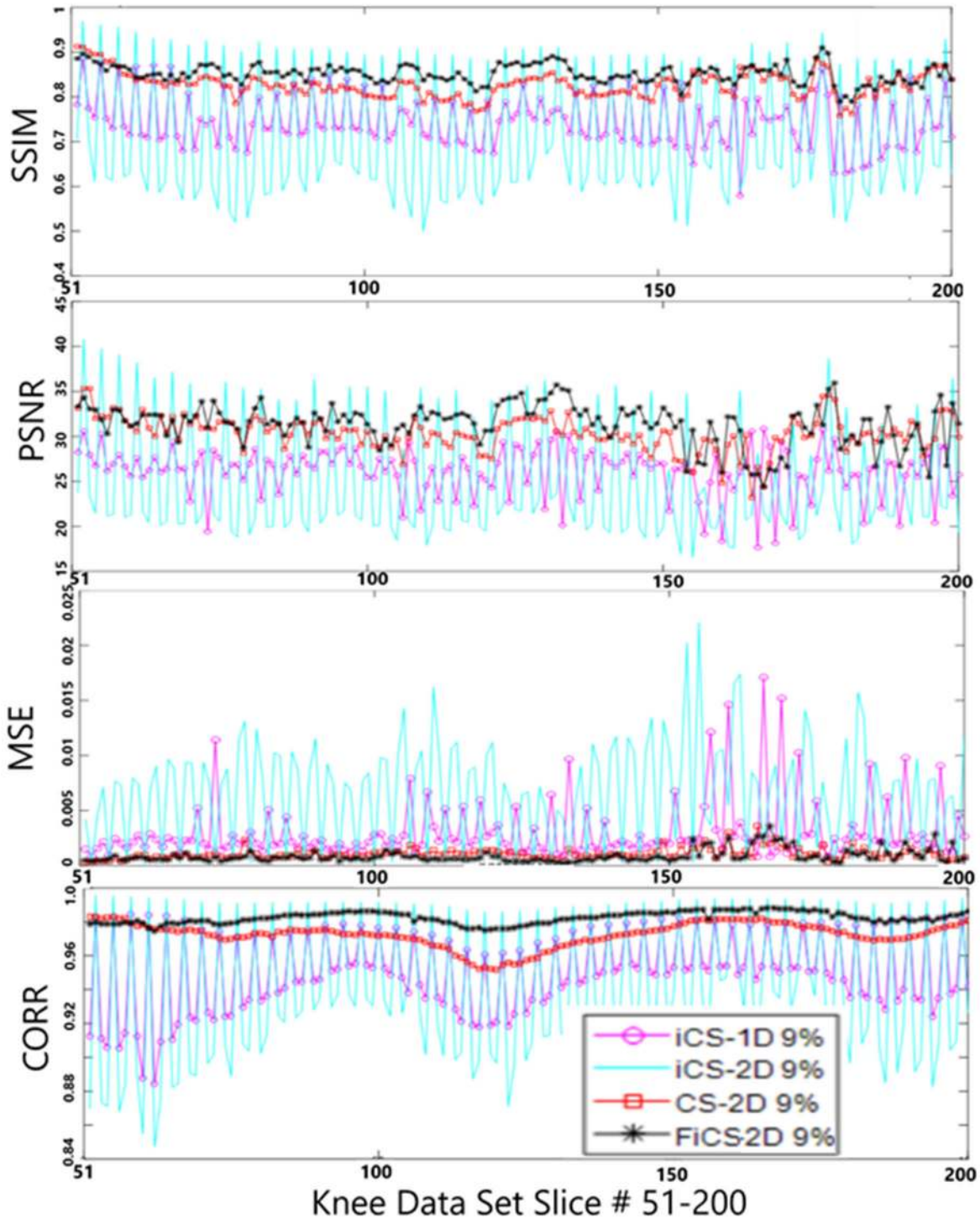

FIGURE 13. Evaluation of the proposed FiCS-2D on 150 slices of knee dataset by comparing it with iCS-1D, iCS-2D and CS-2D using 9% average sampling ratios. It is clear from the graphs that FiCS-2D has a consistent graph like CS with improved results while iCS-1D and 2D shows huge fluctuation in values.

V. DISCUSSION AND CONCLUSION

The proposed FiCS technique is implemented using both 1D and 2D-VRDU masks. Although, 1D mask is more realistic from the current hardware point of view but 2D is best suitable to represent the original k-space data of multi-slice MRI. The 2D under-sampling patterns are not commonly available on clinical scanners at the present time [37] and as with any novel technique within MRI practical implementation requires pulse programming access. There are now a number of research groups who have implemented pulse programs which can perform prospective under-sampling of 2D masks on clinical platforms. For 2D multi-slice MRI, under-sampling in the frequency-encode direction does not reduce acquisition time as the readout direction is acquired very quickly compared to the phase-encode direction.

Our proposed FiCS technique not only preserves the original information in every slice but also gives consistency in the slice wise image quality. The proposed FiCS technique also reduces the sampling ratio to almost half with even improved image quality and information content. The proposed algorithm also beats previous interpolation techniques in terms of computational complexity and processing time. Thus the new sampling and a fast interpolation strategy not only simplifies our proposed technique but also improves the results both qualitatively and quantitatively.

The key findings of this paper are:

- Reduction in scan time, by reducing the under-sampling ratios.
- Improvement in image quality, by preserving maximum samples and information from the original slices.
- Lesser partial volume loss in reconstructed images.
- Reduction in computational complexity and processing time.
- Consistency in slice wise image quality, because of the uniform under-sampling pattern.
- Improved results with even more inter-slice gap data sets.

FUTURE WORK

The proposed interpolation technique can be further explored on different sampling strategies and sampling patterns. The proposed FiCS technique can also be combined with new and improved CS reconstruction techniques for even more improved results and reduced reconstruction time.

REFERENCES

[1] H. Nyquist, "Certain topics in telegraph transmission theory," *Trans. Amer. Inst. Electr. Eng.*, vol. 47, no. 2, pp. 617–644, Apr. 1928.

[2] M. Lustig, J. M. Santos, J.-H. Lee, D. L. Donoho, and J. M. Pauly, *Application of Compressed Sensing for Rapid MR Imaging*. Rennes, France: SPARS, 2005.

[3] M. Zaitsev, J. Maclaren, and M. Herbst, "Motion artifacts in MRI: A complex problem with many partial solutions," *J. Magn. Reson. Imag.*, vol. 42, no. 4, pp. 887–901, Oct. 2015.

[4] P. Paolantonio, R. Ferrari, F. Vecchietti, S. Cucchiara, and A. Laghi, "Current status of MR imaging in the evaluation of IBD in a pediatric population of patients," *Eur. J. Radiol.*, vol. 69, no. 3, pp. 418–424, Mar. 2009.

[5] J. Hamilton, D. Franson, and N. Seiberlich, "Recent advances in parallel imaging for MRI," *Prog. Nucl. Magn. Reson. Spectrosc.*, vol. 101, pp. 71–95, Aug. 2017.

[6] A. Deshmane, V. Gulani, M. A. Griswold, and N. Seiberlich, "Parallel MR imaging," *J. Magn. Reson. Imag.*, vol. 36, pp. 55–72, 2012.

[7] R. Ahmad, H. H. Hu, R. Krishnamurthy, and R. Krishnamurthy, "Reducing sedation for pediatric body MRI using accelerated and abbreviated imaging protocols," *Pediatric Radiol.*, vol. 48, no. 1, pp. 37–49, Jan. 2018.

[8] J. W. Schnaiter *et al.*, "Diagnostic accuracy of an MRI protocol of the knee accelerated through parallel imaging in correlation to arthroscopy," in *RöFo-Fortschritte auf dem Gebiet der Röntgenstrahlen und der bildgebenden Verfahren*. New York, NY, USA: Georg Thieme Verlag KG, 2018, pp. 265–272.

[9] B. Liu, Y. Ming Zou, and L. Ying, "SparseSENSE: Application of compressed sensing in parallel MRI," in *Proc. Int. Conf. Technol. Appl. Biomed.*, May 2008, pp. 127–130.

[10] B. Deka and S. Datta, "Calibrationless joint compressed sensing reconstruction for rapid parallel MRI," *Biomed. Signal Process. Control*, vol. 58, Apr. 2020, Art. no. 101871.

[11] M. Bilal, J. A. Shah, I. M. Qureshi, and K. Kadir, "Respiratory motion correction for compressively sampled free breathing cardiac MRI using smooth ℓ_1-norm approximation," *Int. J. Biomed. Imag.*, vol. 2018, pp. 1–12, Jan. 2018.

[12] M. Bilal, H. Anis, N. Khan, I. Qureshi, J. Shah, and K. A. Kadir, "Reduction of motion artifacts in the recovery of undersampled DCE MR images using data binning and L+S decomposition," *BioMed Res. Int.*, vol. 2019, pp. 1–11, Apr. 2019.

[13] D. L. Donoho, "Compressed sensing," *IEEE Trans. Inf. Theory*, vol. 52, no. 4, pp. 1289–1306, Apr. 2006.

[14] Y. Tsaig and D. L. Donoho, "Extensions of compressed sensing," *Signal Process.*, vol. 86, no. 3, pp. 549–571, Mar. 2006.

[15] E. J. Candes, J. K. Romberg, and T. Tao, "Stable signal recovery from incomplete and inaccurate measurements," *Commun. Pure Appl. Math.*, vol. 59, no. 8, pp. 1207–1223, 2006.

[16] E. J. Candes, M. B. Wakin, and S. P. Boyd, "Enhancing sparsity by reweighted ℓ_1 minimization," *J. Fourier Anal. Appl.*, vol. 14, pp. 877–905, Oct. 2008.

[17] R. Baraniuk, E. Candes, R. Nowak, and M. Vetterli, "Compressive sampling [from the guest editors]," *IEEE Signal Process. Mag.*, vol. 25, no. 2, pp. 12–13, Mar. 2008.

[18] E. J. Candès and M. B. Wakin, "An introduction to compressive sampling [a sensing/sampling paradigm that goes against the common knowledge in data acquisition]," *IEEE Signal Process. Mag.*, vol. 25, no. 2, pp. 21–30, Mar. 2008.

[19] M. Lustig, D. Donoho, and J. M. Pauly, "Sparse MRI: The application of compressed sensing for rapid MR imaging," *Magn. Reson. Med., Off. J. Int. Soc. Magn. Reson. Med.*, vol. 58, no. 6, pp. 1182–1195, 2007.

[20] M. Akcakaya, S. Nam, P. Hu, M. H. Moghari, L. H. Ngo, V. Tarokh, W. J. Manning, and R. Nezafat, "Compressed sensing with wavelet domain dependencies for coronary MRI: A retrospective study," *IEEE Trans. Med. Imag.*, vol. 30, no. 5, pp. 1090–1099, May 2011.

[21] Y. C. Eldar and G. Kutyniok, *Compressed Sensing: Theory and Applications*. Cambridge, U.K.: Cambridge Univ. Press, 2012.

[22] E. Candes, J. Romberg, and T. Tao, "Robust uncertainty principles: Exact signal reconstruction from highly incomplete frequency information," 2004, *arXiv:math/0409186*.[Online]. Available: https://arxiv.org/abs/math/0409186

[23] J. Shah, I. M. Qureshi, J. Proano, and Y. Deng, "Compressively sampled MR image reconstruction using hyperbolic tangent-based soft-thresholding," *Appl. Magn. Reson.*, vol. 46, no. 8, pp. 837–851, Aug. 2015.

[24] J. Shah, I. Qureshi, Y. Deng, and K. Kadir, "Reconstruction of sparse signals and compressively sampled images based on smooth l 1-Norm approximation," *J. Signal Process. Syst.*, vol. 88, no. 3, pp. 333–344, Sep. 2017.

[25] M. Sandilya and S. Nirmala, "Compressed sensing trends in magnetic resonance imaging," *Eng. Sci. Technol., Int. J.*, vol. 20, pp. 1342–1352, 2017.

[26] G. Wang, "A perspective on deep imaging," *IEEE Access*, vol. 4, pp. 8914–8924, 2016.

[27] S. Yu, H. Dong, G. Yang, G. Slabaugh, P. L. Dragotti, X. Ye, F. Liu, S. Arridge, J. Keegan, D. Firmin, and Y. Guo, "Deep de-aliasing for fast compressive sensing MRI," 2017, *arXiv:1705.07137*. [Online]. Available: http://arxiv.org/abs/1705.07137

[28] G. Yang, S. Yu, H. Dong, G. Slabaugh, P. L. Dragotti, X. Ye, F. Liu, S. Arridge, J. Keegan, Y. Guo, and D. Firmin, "DAGAN: Deep de-aliasing generative adversarial networks for fast compressed sensing MRI reconstruction," *IEEE Trans. Med. Imag.*, vol. 37, no. 6, pp. 1310–1321, Jun. 2018.

[29] J. Schlemper, G. Yang, P. Ferreira, A. Scott, L.-A. McGill, Z. Khalique, M. Gorodezky, M. Roehl, J. Keegan, D. Pennell, D. Firmin, and D. Rueckert, "Stochastic deep compressive sensing for the reconstruction of diffusion tensor cardiac MRI," in *Proc. Int. Conf. Med. Image Comput. Comput.-Assist. Intervent*, 2018, pp. 295–303.

[30] S. Ikram, S. Zubair, J. A. Shah, I. M. Qureshi, A. Wahid, and A. U. Khan, "Enhancing MR image reconstruction using block dictionary learning," *IEEE Access*, vol. 7, pp. 158434–158444, 2019.

[31] Ikram, Shah, Zubair, Qureshi, and Bilal, "Improved reconstruction of MR scanned images by using a dictionary learning scheme," *Sensors*, vol. 19, no. 8, p. 1918, Apr. 2019.

[32] J. Yang, Y. Zhang, and W. Yin, "A fast alternating direction method for TVL1-L2 signal reconstruction from partial Fourier data," *IEEE J. Sel. Topics Signal Process.*, vol. 4, no. 2, pp. 288–297, Apr. 2010.

[33] Z. Lai, X. Qu, Y. Liu, D. Guo, J. Ye, Z. Zhan, and Z. Chen, "Image reconstruction of compressed sensing MRI using graph-based redundant wavelet transform," *Med. Image Anal.*, vol. 27, pp. 93–104, Jan. 2016.

[34] W. Zeng, J. Peng, S. Wang, and Q. Liu, "A comparative study of CNN-based super-resolution methods in MRI reconstruction and its beyond," *Signal Process., Image Commun.*, vol. 81, Feb. 2020, Art. no. 115701.

[35] J. Zhu, G. Yang, and P. Lio, "How can we make gan perform better in single medical image super-resolution? A lesion focused multi-scale approach," in *Proc. IEEE 16th Int. Symp. Biomed. Imag. (ISBI)*, Apr. 2019, pp. 1669–1673.

[36] J. Zhu, G. Yang, and P. Lio, "Lesion focused super-resolution," *Proc. SPIE*, vol. 10949, Mar. 2019, Art. no. 109491L.

[37] K. G. Hollingsworth, "Reducing acquisition time in clinical MRI by data undersampling and compressed sensing reconstruction," *Phys. Med. Biol.*, vol. 60, no. 21, pp. R297–R322, Nov. 2015.

[38] Y. Pang and X. Zhang, "Interpolated compressed sensing MR image reconstruction using neighboring slice k-space data," in *Proc. 20th Annu. Meeting ISMRM*, Melbourne, Australia, 2012, p. 2275.

[39] Y. Pang and X. Zhang, "Interpolated compressed sensing for 2D multiple slice fast MR imaging," *PLoS ONE*, vol. 8, no. 2, Feb. 2013, Art. no. e56098.

[40] Y. Pang, J. Jiang, and X. Zhang, "Ultrafast fetal MR imaging using interpolated compressed sensing," in *Proc. Int. Soc. Mag. Reson. Med.*, vol. 2224, 2014.

[41] Y. Pang, B. Yu, and X. Zhang, "Enhancement of the low resolution image quality using randomly sampled data for multi-slice MR imaging," *Quant. Imag. Med. Surg.*, vol. 4, p. 136, Apr. 2014.

[42] G. Shrividya and S. H. Bharathi, "A study of optimum sampling pattern for reconstruction of MR images using compressive sensing," in *Proc. 2nd Int. Conf. Adv. Electron., Comput. Commun. (ICAECC)*, Feb. 2018, pp. 1–6.

[43] J. Huang, L. Wang, and Y. Zhu, "Compressed sensing MRI reconstruction with multiple sparsity constraints on radial sampling," *Math. Problems Eng.*, vol. 2019, pp. 1–14, Feb. 2019.

[44] L. Feng, R. Grimm, K. T. Block, H. Chandarana, S. Kim, J. Xu, L. Axel, D. K. Sodickson, and R. Otazo, "Golden-angle radial sparse parallel MRI: Combination of compressed sensing, parallel imaging, and golden-angle radial sampling for fast and flexible dynamic volumetric MRI," *Magn. Reson. Med.*, vol. 72, no. 3, pp. 707–717, Sep. 2014.

[45] S. Datta, B. Deka, H. U. Mullah, and S. Kumar, "An efficient interpolated compressed sensing method for highly correlated 2D multi-slice MRI," in *Proc. Int. Conf. Accessibility Digit. World (ICADW)*, Dec. 2016, pp. 187–192.

[46] S. Datta and B. Deka, "Magnetic resonance image reconstruction using fast interpolated compressed sensing," *J. Opt.*, vol. 47, no. 2, pp. 154–165, Jun. 2018.

[47] C. Chen and J. Huang, "Compressive sensing MRI with wavelet tree sparsity," in *Proc. Adv. Neural Inf. Process. Syst.*, 2012, pp. 1115–1123.

[48] C. Chen and J. Huang, "Exploiting the wavelet structure in compressed sensing MRI," *Magn. Reson. Imag.*, vol. 32, no. 10, pp. 1377–1389, Dec. 2014.

[49] C. Chen and J. Huang, "The benefit of tree sparsity in accelerated MRI," *Med. Image Anal.*, vol. 18, no. 6, pp. 834–842, Aug. 2014.

[50] J. Huang, S. Zhang, and D. Metaxas, "Efficient MR image reconstruction for compressed MR imaging," *Med. Image Anal.*, vol. 15, no. 5, pp. 670–679, Oct. 2011.

[51] J. Cao, S. Liu, H. Liu, and H. Lu, "CS-MRI reconstruction based on analysis dictionary learning and manifold structure regularization," *Neural Netw.*, vol. 123, pp. 217–233, Mar. 2020.

[52] A. Hirabayashi, N. Inamuro, K. Mimura, T. Kurihara, and T. Homma, "Compressed sensing MRI using sparsity induced from adjacent slice similarity," in *Proc. Int. Conf. Sampling Theory Appl. (SampTA)*, May 2015, pp. 287–291.

[53] S. Datta and B. Deka, "Multi-channel, multi-slice, and multi-contrast compressed sensing MRI using weighted forest sparsity and joint TV regularization priors," in *Soft Computing for Problem Solving*. Singapore: Springer, 2019, pp. 821–832.

[54] S. Datta and B. Deka, "Efficient interpolated compressed sensing reconstruction scheme for 3D MRI," *IET Image Process.*, vol. 12, no. 11, pp. 2119–2127, Nov. 2018.

[55] S. Datta and B. Deka, "Interpolated compressed sensing for calibration-less parallel MRI reconstruction," in *Proc. Nat. Conf. Commun. (NCC)*, Feb. 2019, pp. 1–6.

[56] D. Summers, "Harvard whole brain Atlas: Www.med.harvard.edu/AANLIB/home.html," *J. Neurol., Neurosurgery Psychiatry*, vol. 74, pp. 288–288, 2003.

[57] M. Seitzer, G. Yang, J. Schlemper, O. Oktay, T. Würfl, V. Christlein, T. Wong, R. Mohiaddin, D. Firmin, J. Keegan, D. Rueckert, and A. Maier, "Adversarial and perceptual refinement for compressed sensing MRI reconstruction," in *Proc. Int. Conf. Med. Image Comput. Comput.-Assist. Intervent*, 2018, pp. 232–240.

[58] Z. Wang, A. C. Bovik, H. R. Sheikh, and E. P. Simoncelli, "Image quality assessment: From error visibility to structural similarity," *IEEE Trans. Image Process.*, vol. 13, no. 4, pp. 600–612, Apr. 2004.

[59] A. Hore and D. Ziou, "Image quality metrics: PSNR vs. SSIM," in *Proc. 20th Int. Conf. Pattern Recognit.*, Aug. 2010, pp. 2366–2369.

[60] J. L. Rodgers and W. A. Nicewander, "Thirteen ways to look at the correlation coefficient," *Amer. Statistician*, vol. 42, no. 1, pp. 59–66, Feb. 1988.

MARIA MURAD received the bachelor's degree in telecommunication engineering from the University of Engineering and Technology (UET), Peshawar, Pakistan, in 2010, and the master's degree in electrical engineering from UET, Taxila, Pakistan, in 2012. She is currently pursuing the Ph.D. degree in image processing with International Islamic University Islamabad (IIUI), Pakistan. She has been a Lecturer with International Islamic University Islamabad, since April 2011. Her research interest includes signals and image processing.

MUHAMMAD BILAL received the bachelor's degree in telecommunication engineering from the Institute of Engineering and Technology, Rawalpindi, Pakistan, in 2005, the M.Phil. degree in electronics from Quaid-i-Azam University, Islamabad, Pakistan, in 2008, and the Ph.D. degree from International Islamic University Islamabad (IIUI), Pakistan, in 2019. He is currently a Lecturer with International Islamic University Islamabad. His research interests include sparse signal and biomedical image processing.

ABDUL JALIL received the bachelor's and master's degrees in electronics from Quaid-i-Azam University, Islamabad, Pakistan, in 1986 and 2000, respectively, and the Ph.D. degree in image and signal processing from Mohammad Ali Jinnah University, Pakistan, in 2006. He was with promising chemical and electronic industries, Pakistan, from 1987 to 2002. From 2002 to 2016, he was a Professor (Academician) with the Pakistan Institute of Engineering and Applied Sciences (PIEAS). From 2008 to 2009, he held a postdoctoral position with the University of Sussex, for a period of nine months. He has been a Professor with International Islamic University Islamabad, Pakistan, since February 2016. His research interests include machine vision and signal and image processing.

AHMAD ALI received the bachelor's degree in computer science from UET, Lahore, Pakistan, in 2003, and the M.S. degree in systems engineering and the Ph.D. degree from PIEAS, Islamabad, Pakistan, in 2015. He is the author of a number of publications in image and speech processing. His current research interests include computer vision and artificial intelligence.

KHIZER MEHMOOD received the B.Sc. degree in electronic engineering from International Islamic University Islamabad (IIUI), Pakistan, in 2010, and the M.Sc. degree in electrical engineering from the University of Engineering and Technology, Taxila, Pakistan, in 2013. He is currently pursuing the Ph.D. degree with International Islamic University Islamabad. His research interests include computer vision, visual object tracking, and image processing.

BABER KHAN received the B.S. degree in computer engineering from the COMSATS Institute of Information Technology, Pakistan, in 2010, and the M.S. degree in electrical engineering from the University of Engineering and Technology, Taxila, Pakistan, in 2013. He is currently pursuing the Ph.D. degree in electronic engineering with International Islamic University Islamabad, Pakistan. He is the author of one journal and four conference publications. His research interests include computer vision, pattern recognition, and image processing. He received the awards and honors, include the Campus Silver Medal and the Institute Silver Medal from the B.S. degree in computer engineering.